Jpn. J. Appl. Phys. Vol. 40 (2001) pp. 6391–6395
Part 1, No. 11, November 2001

Simple Formulas for Calculating Wave Propagation and Splitting in Anisotropic Media

Chong-Min CHANG and Han-Ping D. SHIEH
Institute of Electro-Optical Engineering, National Chiao Tung University, Hsinchu, Taiwan 30050, Republic of China

(Received December 20, 2000; accepted for publication July 31, 2001)

A general method for dealing with the propagation of waves in homogeneous anisotropic media is presented. The formulas were derived and applied to determine the reflected and transmitted waves resulting from a plane wave obliquely incident at an interface between two anisotroptic media with arbitrarily oriented principal axes. The validity of the formulas was also demonstrated by calculating the reflection and refraction at a biaxial–biaxial interface.

KEYWORDS: polarization, anisotropic media, biaxial media, compensation films, ray tracing

1. Introduction

Novel optical devices made of optically anisotropic materials exhibit numerous attractive applications, such as polarization sheets, biaxial compensation films, liquid-crystal displays, as well as polarization conversion systems.[1–3] In order to analyze and optimize these optical devices, efficient simulation methods for investigating the light propagation in anisotropic media are necessary. There exist a number of well-known matrix methods developed to study the transmission and reflection characteristics of the uniaxially anisotropic layered films or planar structures.[4–12] However, few methods deal with polarization ray tracing of the general cases of biaxially anisotropic media.[11–13] In this paper, a general formality for systematically manipulating the propagation and splitting of light beams in homogeneous anisotropic materials with the principal axes oriented in arbitrary directions is reported.

2. Formulation

2.1 Wave propagation in anisotropic media

One of the most important phenomena within an anisotropic medium is that, in general, there are two normal modes of distinct refractive indices for a given propagation direction. The *congruence transformation* was employed to simplify the calculation of the refractive indices of an anisotropic medium.[14] Consider a monochromatic plane wave propagating in an anisotropic medium with neither free charge nor current. It is assumed that the medium is homogeneous, nonmagnetic and lossless. In an arbitrary choice of an orthogonal coordinate system, labeled by (x, y, z), the plane wave with the propagation direction $\boldsymbol{u} = [u_x u_y u_z]^{\mathrm{T}}$ and the electrical field $\boldsymbol{E} = [E_x E_y E_z]^{\mathrm{T}}$ must obey the following wave equation:

$$\bar{L}\boldsymbol{E} = \eta\bar{\varepsilon}\boldsymbol{E}, \tag{1}$$

where $\eta = 1/n^2$, n is the refractive index to be determined, $\bar{L}$ is the real symmetric matrix related to the propagation direction:

$$\bar{L} = \begin{bmatrix} u_y^2 + u_z^2 & -u_x u_y & -u_x u_z \\ -u_y u_x & u_z^2 + u_x^2 & -u_y u_z \\ -u_z u_x & -u_z u_y & u_x^2 + u_y^2 \end{bmatrix}, \tag{2}$$

and $\bar{\varepsilon}$ is the dielectric tensor used to specify the optical characteristics of the medium.[5,6] For generality, the medium is assumed to be biaxial and have the oriented principal axes. The dielectric tensor $\bar{\varepsilon}$ in the coordination system (x, y, z) is

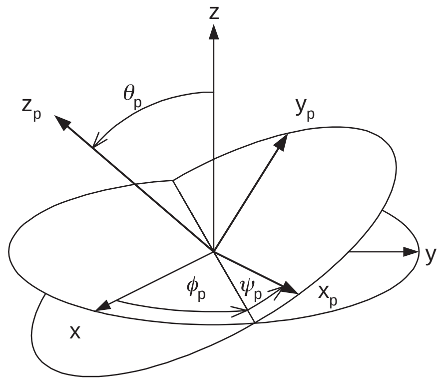

Fig. 1. Orientation of the principal axes $(x_{\mathrm{p}}, y_{\mathrm{p}}, z_{\mathrm{p}})$ described by the Eulerian angles $(\phi_{\mathrm{p}}, \theta_{\mathrm{p}}, \psi_{\mathrm{p}})$.

given by

$$\bar{\varepsilon} = \bar{Q}^{\mathrm{T}} \begin{bmatrix} n_1^2 & 0 & 0 \\ 0 & n_2^2 & 0 \\ 0 & 0 & n_3^2 \end{bmatrix} \bar{Q}, \tag{3}$$

where n_1, n_2, and n_3 are the principal refractive indices, $\bar{Q}$ is a rotation matrix for describing the principal axes $(x_{\mathrm{p}}, y_{\mathrm{p}}, z_{\mathrm{p}})$, and the superscript T indicates the transpose of the matrix. As shown in Fig. 1, the orientation of the principal axes $(x_{\mathrm{p}}, y_{\mathrm{p}}, z_{\mathrm{p}})$ with respect to the coordinate system (x, y, z) can be specified in terms of the Eulerian angles, $(\phi_{\mathrm{p}}, \theta_{\mathrm{p}}, \psi_{\mathrm{p}})$, and thus the matrix $\bar{Q}$ is expressed as

$$\bar{Q} = \begin{bmatrix} \cos\psi_{\mathrm{p}} & \sin\psi_{\mathrm{p}} & 0 \\ -\sin\psi_{\mathrm{p}} & \cos\psi_{\mathrm{p}} & 0 \\ 0 & 0 & 1 \end{bmatrix} \times \begin{bmatrix} 1 & 0 & 0 \\ 0 & \cos\theta_{\mathrm{p}} & \sin\theta_{\mathrm{p}} \\ 0 & -\sin\theta_{\mathrm{p}} & \cos\theta_{\mathrm{p}} \end{bmatrix} \times \begin{bmatrix} \cos\phi_{\mathrm{p}} & \sin\phi_{\mathrm{p}} & 0 \\ -\sin\phi_{\mathrm{p}} & \cos\phi_{\mathrm{p}} & 0 \\ 0 & 0 & 1 \end{bmatrix}. \tag{4}$$

Equation (1) is in the form of a *generalized eigen-equation* containing the two matrix operators, $\bar{L}$ and $\bar{\varepsilon}$, in which η and $\boldsymbol{E}$ are the eigenvalue and eigenvector to be determined. In order to simplify the calculation procedures in solving eq. (1), we employ the techniques of the *congruence transformation*, which is defined by the following transformation matrix:[14)]

$$\bar{C} \equiv \bar{Q}^{\mathrm{T}} \begin{bmatrix} 1/n_1 & 0 & 0 \\ 0 & 1/n_2 & 0 \\ 0 & 0 & 1/n_3 \end{bmatrix}. \tag{5}$$

By substituting $\bar{C}\boldsymbol{F} = \bar{C}[F_x F_y F_z]^{\mathrm{T}}$ for $\boldsymbol{E} = [E_x E_y E_z]^{\mathrm{T}}$, eq. (1) is converted into the form of a *standard eigen-equation* for the single matrix operator $\bar{\Lambda}$ as follows

$$\bar{\Lambda}\boldsymbol{F} = \eta \bar{I}\boldsymbol{F}, \tag{6}$$

where $\bar{I}$ is the 3×3 identity matrix, and $\bar{\Lambda}$ is the real symmetric matrix given by

$$\begin{aligned} \bar{\Lambda} &= \bar{C}^{\mathrm{T}}\bar{L}\bar{C} \\ &= \begin{bmatrix} 1/n_1 & 0 & 0 \\ 0 & 1/n_2 & 0 \\ 0 & 0 & 1/n_3 \end{bmatrix} \bar{Q} \\ &\times \begin{bmatrix} u_y^2 + u_z^2 & -u_x u_y & -u_x u_z \\ -u_y u_x & u_z^2 + u_x^2 & -u_y u_z \\ -u_z u_x & -u_z u_y & u_x^2 + u_y^2 \end{bmatrix} \bar{Q}^{\mathrm{T}} \\ &\times \begin{bmatrix} 1/n_1 & 0 & 0 \\ 0 & 1/n_2 & 0 \\ 0 & 0 & 1/n_3 \end{bmatrix}, \end{aligned} \tag{7}$$

In addition, the vector $\boldsymbol{F} = [F_x F_y F_z]^{\mathrm{T}}$ is related to the electrical field $\boldsymbol{E} = [E_x E_y E_z]^{\mathrm{T}}$ and is written as

$$\boldsymbol{F} = \bar{C}^{-1}\boldsymbol{E} = \begin{bmatrix} n_1 & 0 & 0 \\ 0 & n_2 & 0 \\ 0 & 0 & n_3 \end{bmatrix} \bar{Q} \begin{bmatrix} E_x \\ E_y \\ E_z \end{bmatrix}. \tag{8}$$

Apparently, this transformation matrix $\bar{C}$ gives another choice for the coordinate system, which is a combination of a pure rotation and scaling, such that eq. (1) is reduced into a simpler equation for solving the associated eigen problems.

For nontrivial solutions of eq. (6) to exist, the characteristic polynomial of the matrix $\bar{\Lambda}$ must vanish, leading to the following *cubic* polynomial equation:

$$|\eta\bar{I} - \bar{C}^{\mathrm{T}}\bar{L}\bar{C}| = \eta(\eta^2 - 2V\eta + W) = 0, \tag{9}$$

where V and W are the coefficients of the polynomial equation. In eq. (9), the constant term is zero because of $|\bar{L}| = 0$. On the other hand, the constants, V and W, are determined by the matrix elements Λ_{uv} $(u, v = x, y, z)$ of the matrix $\bar{\Lambda}$, and are given by

$$V = \frac{1}{2}(\Lambda_{xx} + \Lambda_{yy} + \Lambda_{zz}), \tag{10}$$

$$\begin{aligned} W = &\Lambda_{yy}\Lambda_{zz} + \Lambda_{zz}\Lambda_{xx} + \Lambda_{xx}\Lambda_{yy} - \Lambda_{yz}\Lambda_{zy} \\ &- \Lambda_{zx}\Lambda_{xz} - \Lambda_{xy}\Lambda_{yx}. \end{aligned} \tag{11}$$

It should be noted that the zero root of eq. (9) corresponds to the theoretical solution with $n = \infty$, and should be dropped. While the other two nonzero roots, $V \pm \sqrt{V^2 - W}$, lead to the following formulas of the refractive indices:

$$n_{\mathrm{inner}} = \sqrt{\frac{V - \sqrt{V^2 - W}}{W}}, \tag{12}$$

$$n_{\mathrm{outer}} = \sqrt{\frac{V + \sqrt{V^2 - W}}{W}}, \tag{13}$$

where V and W are defined by eqs. (10) and (11), respectively. Consequently, there are two normal modes for each propagation direction in an anisotropic medium: one propagates with the refractive index n_{inner}, and the other propagates with n_{outer}. It is clear from eqs. (12) and (13) that the value of n_{inner} is less than n_{outer}, thus the front is referred to as the "inner-sheet" reflective index, and the latter as the "outer-sheet" refractive index. Once the refractive indices, n_{inner} and n_{outer}, are determined, the corresponding polarization vectors can then be obtained from the eigenvectors of eq. (6) to complete the solutions.

2.2 *Reflection and refraction at interfaces*

The calculations of reflected and refracted waves at a planar interface between two generally oriented anisotropic media are other fundamental issues in the polarization ray tracing. We apply formulas developed in §2.1 and impose boundary conditions to obtain a general method for computing the propagation directions of these splitting waves. The coordination system and symbols used for our formulas are shown in Fig. 2. For the sake of convenience, the z-axis direction of the coordinate system, labeled by (x, y, z), is taken to be perpendicular to the interface and the polar and azimuth angles of the wavevector are used to specify the propagation direction. Consider a plane wave incident upon the interface with the following wavevector:

$$\boldsymbol{k}_{\mathrm{i}} = \frac{2\pi}{\lambda} n_{\mathrm{i}} [\sin\theta_{\mathrm{i}}\cos\phi_{\mathrm{i}} \quad \sin\theta_{\mathrm{i}}\sin\phi_{\mathrm{i}} \quad \cos\theta_{\mathrm{i}}]^{\mathrm{T}}, \tag{14}$$

where λ is the wavelength, n_{i} is the refractive index given by eq. (12) or (13), θ_{i} is the polar angle, and ϕ_{i} is the azimuth angle. Similarly, the wavevectors of the reflected and refracted waves, $\boldsymbol{k}_{\mathrm{r}}$ and $\boldsymbol{k}_{\mathrm{t}}$, are expressed as

$$\boldsymbol{k}_{\mathrm{r}} = \frac{2\pi}{\lambda} n_{\mathrm{r}} [\sin\theta_{\mathrm{r}}\cos\phi_{\mathrm{r}} \quad \sin\theta_{\mathrm{r}}\sin\phi_{\mathrm{r}} \quad \cos\theta_{\mathrm{r}}]^{\mathrm{T}}, \tag{15}$$

$$\boldsymbol{k}_{\mathrm{t}} = \frac{2\pi}{\lambda} n_{\mathrm{t}} [\sin\theta_{\mathrm{t}}\cos\phi_{\mathrm{i}} \quad \sin\theta_{\mathrm{t}}\sin\phi_{\mathrm{i}} \quad \cos\theta_{\mathrm{t}}]^{\mathrm{T}}. \tag{16}$$

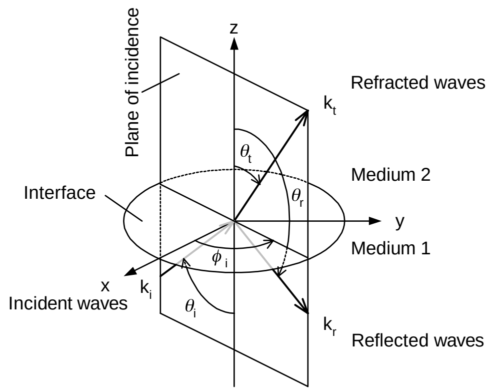

Fig. 2. Propagation directions of the incident, reflected, and refracted waves specified by the angles $(\phi_{\mathrm{i}}, \theta_{\mathrm{i}})$, $(\phi_{\mathrm{r}}, \theta_{\mathrm{r}})$, and $(\phi_{\mathrm{t}}, \theta_{\mathrm{t}})$.

Here the subscripts i, r, and, t in the above equations denote the components of the incident, reflected and refracted waves, respectively. Note that the azimuth angles of the reflected and refracted waves are identical to the value of ϕ_i, while their polar angles, θ_r and θ_t, are the unknown variables to be determined. The boundary condition requires that the phases of the fields on both sides of the interface must match. Applying the boundary condition, together with eqs. (12) and (13) for the refractive indices, we obtain the following four equations that determine the polar angles, θ_r and θ_t:

$$n_\mathrm{i}\sin(\theta_\mathrm{i}) = \begin{cases} \sqrt{\dfrac{V_1 - \sqrt{V_1^2 - W_1}}{W_1}}\sin(\theta_\mathrm{r}) & (17) \\ \sqrt{\dfrac{V_1 + \sqrt{V_1^2 - W_1}}{W_1}}\sin(\theta_\mathrm{r}), & (18) \end{cases}$$

$$n_\mathrm{i}\sin(\theta_\mathrm{i}) = \begin{cases} \sqrt{\dfrac{V_2 - \sqrt{V_2^2 - W_2}}{W_2}}\sin(\theta_\mathrm{t}) & (19) \\ \sqrt{\dfrac{V_2 + \sqrt{V_2^2 - W_2}}{W_2}}\sin(\theta_\mathrm{t}), & (20) \end{cases}$$

where $\sqrt{(V_\rho \pm \sqrt{V_\rho^2 - W_\rho})/W_\rho}$ $(\rho = 1, 2)$ are the refractive indices of the media. The subscripts 1 and 2 denote the parameters in medium 1 and medium 2, respectively. In addition, it should be noted that the values of V_ρ and W_σ $(\rho = 1, 2)$, in general, vary with the propagation direction of the wave and the dielectric tensor of the medium. For the incident wave with the specified angles $(\phi_\mathrm{i}, \theta_\mathrm{i})$ and refractive index n_i, the polar angles of the reflected waves and the refracted waves, θ_r and θ_t, can be solved numerically from eqs. (17)–(20), respectively. Equations (17)–(20) are in a form similar to Snell's law, and yet allow systematic manipulation of light splitting at the interface between two biaxially anisotropic media.

3. Numerical Results

Applying the formulas developed in the preceding sections, we analyzed the general case of an oblique plane wave incident upon a biaxial–biaxial interface. Figure 2 is a schematic diagram of the arrangement and the chosen coordination system. In the calculation, the optical parameters of the two biaxial media are taken from ref. 9, in which medium 1 and medium 2 have the same principal refractive indices: $n_1 = 1.2$, $n_2 = 1.7$, and $n_3 = 2.2$, but their principal axes are oriented differently: $\phi_\mathrm{p} = 90°$, $\theta_\mathrm{p} = 70°$, and $\psi_\mathrm{p} = -90°$ for medium 1, and $\phi_\mathrm{p} = 30°$, $\theta_\mathrm{p} = 30°$, and $\psi_\mathrm{p} = 30°$ for medium 2. The normal (wavevector) surfaces of medium 1 and medium 2 were calculated using eqs. (12) and (13), and are shown in Figs. 3(a) and 3(b), respectively. It is seen that each normal surface of the medium is composed of two sheets, in which the inner-sheet given by eq. (12) is entirely contained by the outer-sheet given by eq. (13).

Considering the polar angle of incidence θ_i to vary from 0° to 90° and the azimuth angle $\phi_\mathrm{i} = 0°$, we calculated the polar angles of the reflected and refracted waves by solving eqs. (17)–(20) numerically. According to the description in §2.1, there exist two normal modes (inner-sheet or outer-sheet) of the incident wave for a specified propagation direction, thus two cases were analyzed separately. First, we examined the reflection and refraction of a plane wave with the inner-sheet refractive index given by eq. (12). The polar angles of the reflected and refracted waves are shown in Figs. 4(a) and 4(b), where the dashed and solid curves denote the inner- and outer-sheet solutions, respectively. As the incidence angle θ_i varies from 0° to 90°, eqs. (17)–(20) yield two backward-propagating waves and two forward-propagating waves, resulting in the familiar phenomena of double reflection and refraction at the boundary.

Next, we calculated the reflected and refracted waves excited by the incidence of a plane wave with the outer-sheet refractive index given by eq. (13). The polar angles of these waves are shown in Figs. 5(a) and 5(b). Again, the double reflection and refraction occur, as the incidence angle θ_i in-

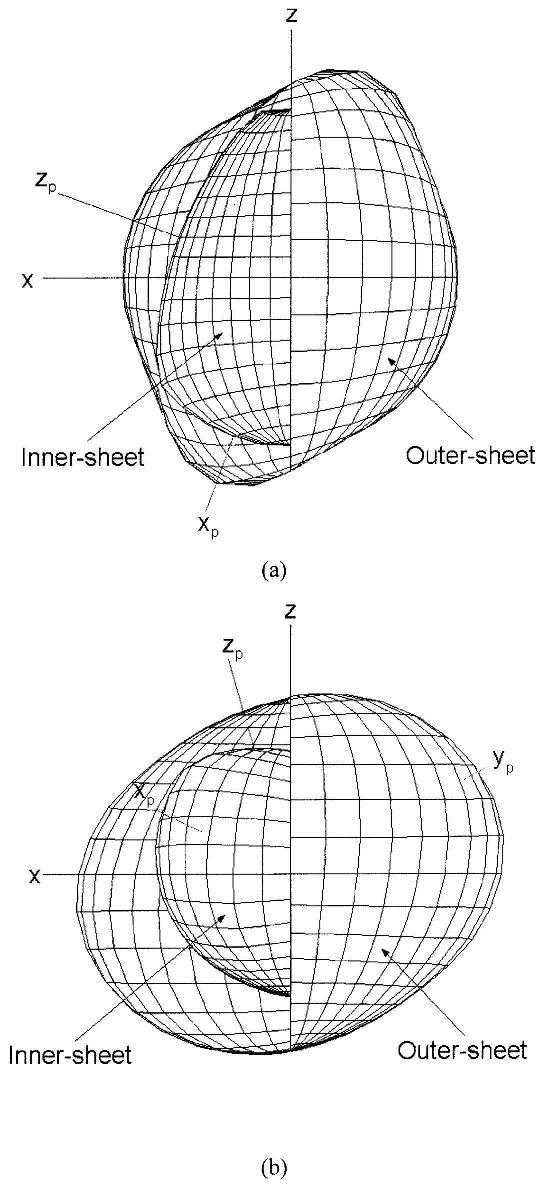

Fig. 3. Surface plots of the inner- and outer-sheet normal (wavevector) surfaces in (a) medium 1 ($n_1 = 1.2$, $n_2 = 1.7$, $n_3 = 2.2$; $\phi_\mathrm{p} = 90°$, $\theta_\mathrm{p} = 70°$, $\psi_\mathrm{p} = -90°$) and (b) medium 2 ($n_1 = 1.2$, $n_2 = 1.7$, $n_3 = 2.2$; $\phi_\mathrm{p} = 30°$, $\theta_\mathrm{p} = 30°$, $\psi_\mathrm{p} = 30°$).

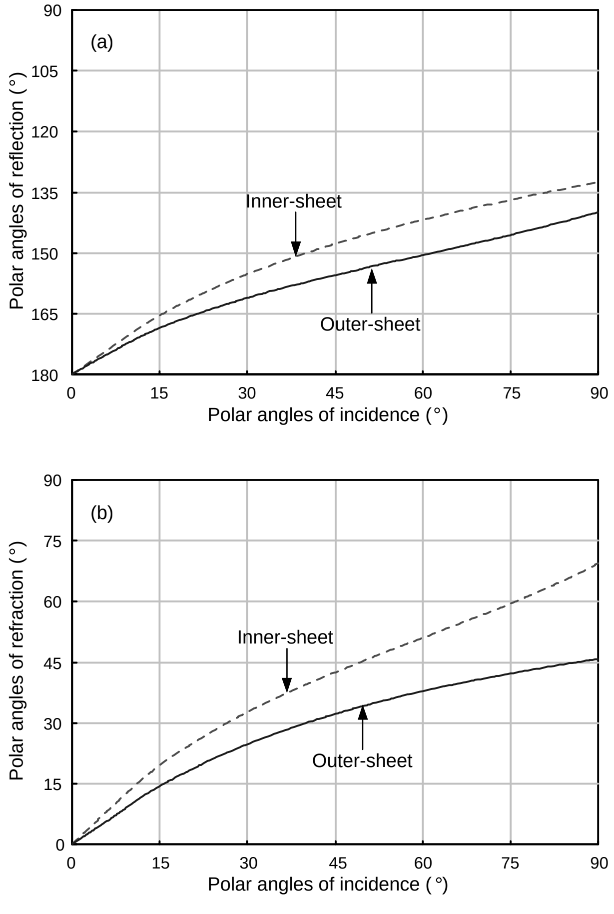

Fig. 4. Polar angles of (a) the reflected and (b) refracted waves versus the incidence angle of the inner-sheet wave.

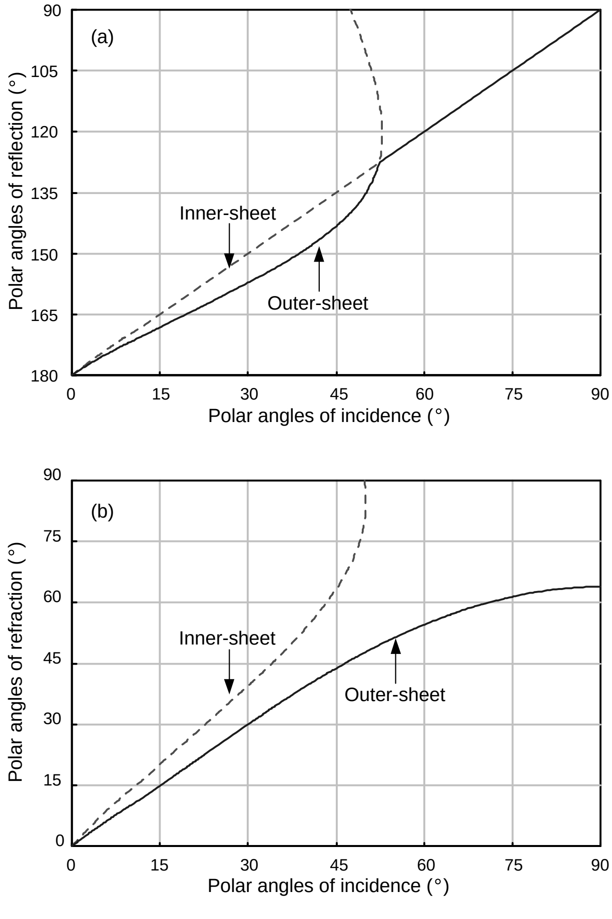

Fig. 5. Polar angles of (a) the reflected and (b) refracted waves versus the incidence angle of the outer-sheet wave.

creases from 0° to 49°. Notice that when the incidence angle θ_i is around 50°, eqs. (17) and (19) have multiple roots, leading to "triple" reflection and "triple" refraction at the boundary. In this special case, three waves propagate backward, and three waves propagate forward. If the incident angle θ_i increases further, there exist one reflected wave in medium 1, and one refracted wave in medium 2.

To illustrate the latter two special cases, the wavevectors for the incidence angles of 50° and 60° are plotted in Figs. 6(a) and 6(b), along with the cross sections of the normal surfaces on the plane of incidence. As shown in Fig. 6(a), the inner-sheet of medium 1 yields two backward-propagation wavevectors, and the outer-sheet yields one, thus giving rise to three reflected waves. In medium 2, the inner-sheet provides two forward-propagation wavevectors, and the outer-sheet causes one, thus leading to three refracted waves. For the special case shown in Fig. 6(b), the tangential component of the incident wavevector exceeds those of the inner-sheets of medium 1 and medium 2, and, consequently, the waves related to the inner-sheets do not exist. Thus, only the reflected and refracted waves associated with the outer-sheets are obtained.

In order to investigate the phenomena at the biaxial–biaxial interfaces, a prism assembly that consists of two triangular wedges of biaxial materials is suggested to be used in carrying out the associated experiment.[15] The two triangular wedges are cemented together with their optical axes oriented to each other for providing the biaxial–biaxial interface. Using the proposed simulation method, the output splitting angles, retardations, and interference fringes caused by this prism can be analyzed. Additionally, we are planning to fabricate the biaxial prisms and develop the cement technology. The analysis and experimental results will be reported in the near future.

4. Conclusions

We have developed a general formality for investigating the propagation of light in homogeneous anisotropic media. By using the congruence transformation, simple formulas were derived to calculate the propagation modes associated with a specified propagation direction. In addition, the equations for determining the reflection and refraction waves at a plane interface between two biaxially anisotropic media were also obtained. The formulas were demonstrated by the general case of a plane wave obliquely incident at a biaxial–biaxial interface, showing that the procedure works well for an arbitrary angle of incidence. The proposed approach provides a general and systematic way to analyze the propagation of plane waves, so that the results should be useful for calculating light paths through optical systems containing anisotropic media.

Acknowledgements

The authors acknowledge Drs. Hugo Cornelissen, Saskia Blom, Dick de Boer, and Jos van Haaren of Philips Research Laboratories, Eindhoven, Netherlands, for useful discussions. We gratefully appreciate the generous support from Philips

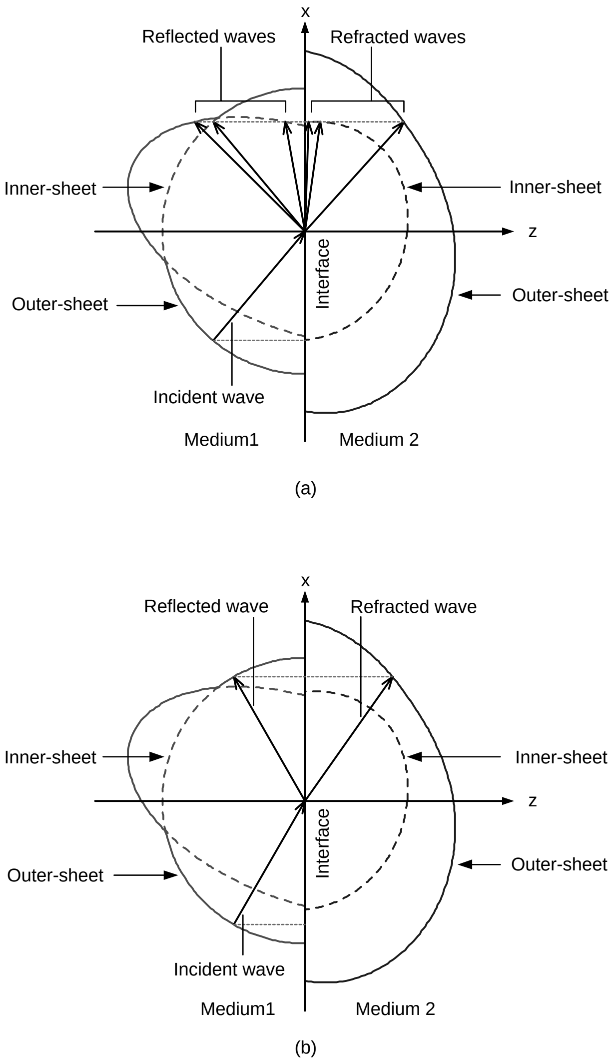

Fig. 6. Plots of the wavevectors for the incidence angles of (a) 50° and (b) 60° along with the cross sections of the normal surfaces on the plane of incidence.

Innovation Center of Taipei and Philips Electronics Inc., Ltd., Taiwan, Republic of China. This work was also partially supported by National Science Council of Republic of China under contract No. NSC 89-2215-E009-082.

1) C.-J. Chen, A. Lien and M. I. Nathan: Jpn. J. Appl. Phys. **35** (1996) L1204.
2) P. van de Witte, J. van Haaren, J. Tuijtelaars, S. Stallinga and J. Lub: Jpn. J. Appl. Phys. **38** (1999) 748.
3) C.-M. Chang and H.-P. D. Shieh: Jpn. J. Appl. Phys. **39** (2000) 6580.
4) D. W. Berreman: J. Opt. Soc. Am. **62** (1972) 502.
5) P. Yeh: J. Opt. Soc. Am. **72** (1982) 507.
6) P. Yeh: J. Opt. Soc. Am. A **10** (1993) 966.
7) Quan-Ting Liang: Appl. Opt. **29** (1990) 1008.
8) S. C. McClain, L. W. Hillman and R. A. Chipman: J. Opt. Soc. Am. A **10** (1993) 2371.
9) S. C. McClain, L. W. Hillman and R. A. Chipman: J. Opt. Soc. Am. A **10** (1993) 2383.
10) E. Georgieva: J. Opt. Soc. Am. A **12** (1995) 2203.
11) G. Beyerle and I. S. MacDermid: Appl. Opt. **37** (1998) 7947.
12) E. Cojocaru: Appl. Opt. **38** (1999) 4004.
13) G. D. Landry and T. A. Maldonado: J. Opt. Soc. Am. **12** (1995) 2048.
14) G. Strang: *Linear Algebra and its Applications 1976* (Academic Press, New York, 1976) p. 248.
15) C. C. Montarou and T. K. Gaylord: Appl. Opt. **38** (1999) 6604.